

Energy & Environmental Science

Accepted Manuscript



This is an *Accepted Manuscript*, which has been through the Royal Society of Chemistry peer review process and has been accepted for publication.

Accepted Manuscripts are published online shortly after acceptance, before technical editing, formatting and proof reading. Using this free service, authors can make their results available to the community, in citable form, before we publish the edited article. We will replace this *Accepted Manuscript* with the edited and formatted *Advance Article* as soon as it is available.

You can find more information about *Accepted Manuscripts* in the [Information for Authors](#).

Please note that technical editing may introduce minor changes to the text and/or graphics, which may alter content. The journal's standard [Terms & Conditions](#) and the [Ethical guidelines](#) still apply. In no event shall the Royal Society of Chemistry be held responsible for any errors or omissions in this *Accepted Manuscript* or any consequences arising from the use of any information it contains.

COMMUNICATION

Supercapacitor/biofuel cell hybrids based on wired enzymes on carbon nanotube matrices: Autonomous reloading after high power pulses in neutral buffered glucose solutions

Cite this: DOI: 10.1039/x0xx00000x

Received 00th January 2012,
Accepted 00th January 2012

DOI: 10.1039/x0xx00000x

www.rsc.org/

C. Agnès^a, M. Holzinger^a, A. Le Goff^a, B. Reuillard^a, K. Elouarzaki^a, S. Tingry^b and Serge Cosnier^{*a}

We report an original setup using carbon nanotube matrices as supercapacitor where redox enzymes serve for continuous charging of the capacitors. High currents can be delivered under short pulse discharges. This supercapacitor/biofuel cell hybrid system remains stable for at least 40 000 pulses of 2 mW.

Electrochemical supercapacitors can be seen as the bridge between batteries and classic capacitors due to their properties to store high energy densities combined with rapid charge/discharge cycles. They are of particular interest when high power has to be delivered or stored within very short time¹⁻³. These characteristics opened a wide variety of applications for supercapacitors that ranges from the power supply of low power consuming mobile devices (several mW) to their use in the automotive sector (several kW).²

Supercapacitors usually contain 2 porous electrodes where both electrodes are placed in a highly ionic solution, the electrolyte, and are separated by a membrane.^{4,5} The specific surface area and the pore sizes play an important role for the performances of these supercapacitors. Depending on the design of the electrodes, the energy is stored in different manners that lead to different types of supercapacitors. Double layer capacitors, usually made out of porous carbon materials, are based on electrostatic storage of electrical energy. Pseudocapacitors store the electrical energy via electrochemical redox reactions and consist generally of metal oxide electrodes or conducting polymers^{6,7}. In case of double layer capacitors, conductive nanostructured materials became highly appropriate candidates for such setups⁵. Nanostructured carbons like activated carbon, carbon nanotubes (CNTs)⁵, or graphene^{8,9} are mostly used as electrode material of choice. For the electrochemical storage of energy, beside RuO₂ and other transition metal oxides¹⁰, hydrogenated TiO₂ nanotubes became recently prominent examples for the construction of high performance supercapacitors with extremely short charging time and high capacitance¹¹.

Except few examples¹², all supercapacitors need to be charged by an external power source. As a consequence, hybrid systems, coupling such supercapacitors with batteries or fuel cells, were proposed.¹³

A particular challenge is when pulsed energy is needed in implantable electronic devices such as pacemakers, neurostimulators, or defibrillators where supercapacitors play an important role.¹⁴ The possibility to recharge implanted supercapacitors with an internal energy source could therefore represent a clear improvement.

Glucose/O₂ biofuel cells are of particular interest for harvesting energy from glucose and oxygen, both present in body fluids¹⁵⁻¹⁷. Such biofuel cells rely on redox enzymes wired on electrodes to harvest power by oxidizing specifically the “fuel” (glucose) at the bioanode and reducing O₂ at the biocathode¹⁸. The possibility to produce electric power out of living organisms was realized by insertion of the biofuel cell electrodes in a rabbit ear¹⁹, cockroaches,²⁰ clams²¹, snail²², lobsters²³, or by deposition of the bioelectrodes onto the exposed cremaster tissue of a rat²⁴. A micro biofuel cell was successfully implanted in a vein of a rat²⁵. Finally, a completely surgically implanted glucose fuel cell in the rat’s abdomen could produce enough energy to flash several times a LED and to power a digital thermometer by charging an external capacitor²⁶. CNTs were mostly used as electrode material for these enzymatic biofuel cells, thanks to their high specific surface, high conductivity and high enzyme wiring efficiency²⁷. CNTs allow direct wiring of redox enzymes like glucose oxidase (GOx), tyrosinase and laccase (Lacc) where the charge transfer, involved in the biocatalytic redox process, are transferred to an external circuit via the carbon nanotube matrix^{28,29}. The conductivity, surface area, and the formation of mesoporous structures in bulk are beneficial attributes of these carbon nanotubes also in supercapacitors³⁰.

In this context, we propose an original hybrid system using a CNTs matrix as supercapacitors and as electrode material for a biofuel cell setup. This supercapacitor/biofuel cell hybrid enabled high power discharge cycles where the CNT matrix was continuously recharged via biocatalytic energy conversion.

The CNT/enzyme matrix was formed by compression of the CNTs (MWCNTs, purchased from Nanocyl (>95% purity, 10nm diameter)) in presence of enzymes under applied force of 1×10^4 N

in a hydraulic press (Perkin–Elmer, Germany)²⁹. For the enzyme/CNT anode, MWCNTs (200 mg), GOx from *Aspergillus Niger* (50 mg), and catalase from bovine liver (30 mg) were ground with water (1 mL) until a homogeneous paste like composite was obtained. Catalase was added to consume the side product H_2O_2 formed by unwired GOx which can have a deleterious effect for GOx during mid- and long-term measurements. Furthermore, the disproportionation of hydrogen peroxide by catalase leads to local depletion of oxygen favoring improved electron transfer kinetics between GOx and the CNT matrix. Finally, this mixture was then compressed to give disks with 6 mm thickness and 13 mm in diameter. The same procedure was applied for the enzyme/CNT cathode by using Laccase from *Trametes Versicolor* (70 mg) instead of GOx and catalase.

The obtained pellets were contacted with wires using carbon paste. By leaving one side (surface 1.3 cm^2) exposed to the electrolyte solution, the rest of the electrode was covered with insulating water-repellent glue. Both electrodes were finally connected to an external circuit (Biologic VMP3 Multi potentiostat). No membrane was used to separate anode and cathode. The compressed CNT matrix favors direct electron transfer (DET) with the redox enzymes. At the bioanode, wired GOx catalyzes the oxidation of glucose to gluconolactone releasing two electrons which are transferred to the CNT matrix (Figure 1, left). Furthermore, such compression might also lead to the destruction of some GOx enzymes where the released FAD can act as mediator for the electron transfer. This possibility has to be considered since DET and FAD mediated electron transfer lead an identical open circuit potential (OCP) and can therefore not be distinguished. For unwired GOx and its regeneration by oxygen forming hydrogen peroxide, the enzyme catalase is added to convert H_2O_2 to water and oxygen²⁹. At the biocathode, Lacc catalyzes the reduction of oxygen to water in a four-electron step. These electrons are supplied by the surrounding CNT matrix. The specific surface of the CNT matrix was determined by Brunauer–Emmett–Teller (BET) measurements: N_2 adsorption–desorption isotherms were acquired using a Micromeritics ASAP 2020 instrument. The samples were previously outgassed at $200\text{ }^\circ\text{C}$ for 2 h. Average pore diameter size was calculated via the Barrett–Joyner–Halenda (BJH) method³¹. A specific surface of $280\text{ m}^2\cdot\text{g}^{-1}$ with an average pore size of 13 nm was determined. The resulting bioelectrodes were placed in an air-saturated electrolyte ($0.2\text{ mol}\cdot\text{L}^{-1}$ phosphate buffer solution, pH 7 at room temperature) containing $200\text{ mmol}\cdot\text{L}^{-1}$ glucose. The supercapacitor performances under pulsed

discharge conditions and the biocatalytic recharge cycles were studied.

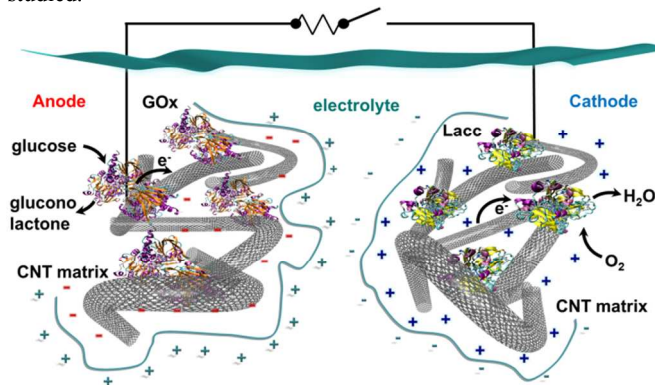


Figure 1. Scheme of the electrochemical double layer supercapacitor – biofuel cell hybrid system.

The bioelectrodes were stored for 3 days in these solutions to obtain an equilibrium concentration of glucose and oxygen throughout the porous CNT matrix and the complete charging of the capacitance. This stabilization of the bioelectrodes was monitored by measuring the open circuit voltage (OCV) which reached in average a value around $1.0\text{ (+/-}0.1\text{)}\text{ V}$ after three days storage. The obtained OCV values are close to the sum of the optimal OCPs of each bioelectrode, *i.e.* around -0.35 V for the GOx/CNT and around $+0.6\text{ V}$ for the Lacc/CNT electrode.

The supercapacitor/biofuel cell hybrid device was then evaluated by applying several discharge cycles at defined current. After each discharge pulse, the hybrid system recovered itself due to the continuous energy conversion of the biocatalysts in presence of glucose and oxygen. Figure 2A shows the evolution of the capacitor voltage with different current pulses during 10 ms, ranging from 1 mA to 10 mA.

When a current pulse is applied, a clear voltage drop is observed whose intensity depends on the applied current. After the pulse (10 ms), the potential returns quickly to its initial value.

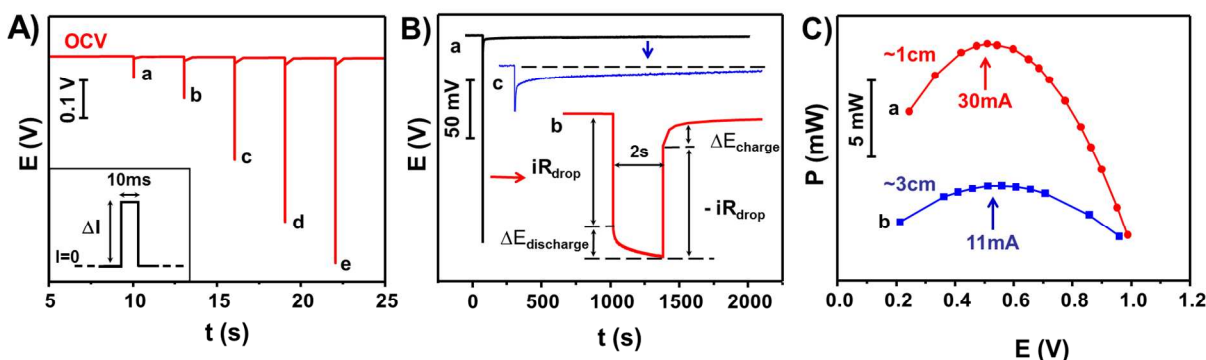


Figure 2. A) Measured voltage drops by applying different current pulses: a) 1 mA; b) 2 mA; c) 5 mA; d) 8 mA; e) 10 mA during 10 ms (principle see inset). B) a) Current pulse of 3 mA during 2 s. b) Zoom at the voltage drop peak, and c) zoom at the partial recovering of the cell voltage during 2000 s. C) Power-Voltage profiles mapped after current pulses from 0.1 mA to 45 mA at different electrode distances a) 1 cm and b) 3 cm. The measurements were performed in air saturated PBS ($0.2\text{ mol}\cdot\text{L}^{-1}$, pH 7) containing $0.2\text{ mol}\cdot\text{L}^{-1}$ glucose at room temperature.

COMMUNICATION

To get more insight in the nature of this voltage drop, we measured the evolution of the voltage for a 2 s discharge pulse of 3 mA with a recharge period of 2 000 s (Figure 2Ba). Figure 2Bb shows a magnification of this peak where a common internal ohmic drop can initially be observed. This drop is followed by a slower voltage decrease which is assigned to the discharge of the capacitance ($\Delta E_{\text{discharge}}$). After discharge, the voltage recovers very fast ($-iR_{\text{drop}}$) followed by a slow increase of the voltage due to the recharge of the capacitance by the bioelectrocatalytic reactions (ΔE_{charge}). It has to be noted that the initial OCV is not completely recovered after this 2 s pulse of 3 mA (Figure 2Bc). This is most likely due to the slow diffusion of glucose and oxygen to the biocatalytic material.

To evaluate the influence of the distance between the negative and the positive electrode, we placed the 2 electrodes at a distance of 1 cm and 3 cm. We applied several current pulses during 10 ms each within a current range from 0.1 mA to 45 mA. This short discharge time was chosen to allow faster recovering of the OCV. The voltage drops were measured for each pulse and the obtained power was plotted for each potential. Figure 2C presents the power profile corresponding to the biofuel cell setup. The setup with shorter electrode distance (1 cm) delivers lower voltage drops, inducing at 0.5 V an effective power around 3 times higher (16 mW) than the power delivered (6 mW at 0.5 V) using the setup with longer distance in between the electrodes (3 cm). This is in correlation with classical supercapacitors where the electrodes are usually separated by highly ion conductive porous membranes with a thickness of less than 1 mm. The apparent maximum power of 16 mW at 0.5 V is obtained for the setup with 1 cm electrode distance when a 30 mA-current pulse is applied (Figure 2C).

As for common energy storage or harvesting devices, the power increase with reduced electrode distances is directly related to the reduced electrolyte resistivity giving $R_{\text{electrolyte}} = 45 \Omega$ (3 cm) and $R_{\text{electrolyte}} = 15 \Omega$ (1 cm).

In order to verify the stability of our system, we applied current pulses of 3 mA for 10 ms every 10 s during 5 days. The electrodes were placed in an electrolyte solution containing 200 mmol.L⁻¹ glucose and oxygen (air saturated solution). The evolution of the voltage was monitored for each pulse. The supercapacitor/biofuel cell hybrid could recover after each discharge for 10 s (Figure 3). During the first day, the voltage of our setup decreases until equilibrium between the charge/discharge cycle and the substrate diffusion is reached. Then stabilization occurs at 0.67 V (Figure 3Ba) and is maintained for the rest of the experiment (4 further days). Since the charging of the CNT matrix is directly correlated to the biocatalytic energy conversion, the initial voltage decrease is most likely due to the diffusion constant of glucose and oxygen throughout the CNT electrode. This led, in the beginning of the experiment, to a partial consumption of the stored energy until equilibrium was reached after one day.

In order to demonstrate that the consumed energy is recovered by the biocatalytic energy conversion of glucose and O₂, the electrodes were simply placed, after these 5 days of continuous charge-discharge cycles, in an electrolyte solution (PBS, 0.2 M, pH 7) that

did not contain glucose (Figure 3Bb). At the beginning, the voltage of the supercapacitor is slightly higher than during the stabilized charge/discharge cycles due to the remaining glucose inside the CNT matrix. This led to a further charging of the capacity via its biocatalytic conversion to electric energy during the change of electrolyte solution. Without the presence of glucose, the voltage decreases linearly during the charge/discharge cycles. This shows clearly that no recharging of the capacity takes place and represents the proof of concept of our supercapacitor/biofuel cell hybrid system.

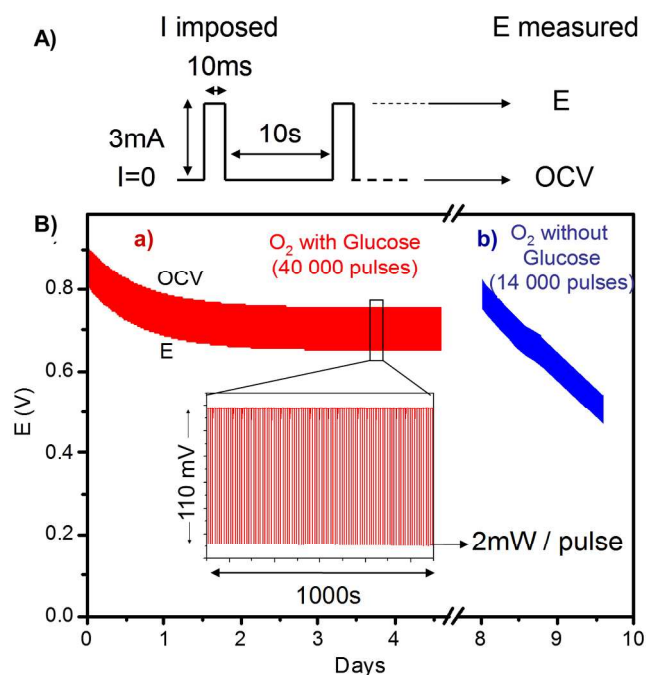


Figure 3. A) Experimental setup: measurement of ΔE for each discharge pulse of 3 mA for 10 ms every 10 s B) Long term stability test of the supercapacitor/biofuel cell hybrid system under discharge conditions as in A) applying a) 40 000 pulses of 2 mW in air saturated PBS (0.2 mol.L⁻¹, pH 7) containing 0.2 mol.L⁻¹ glucose at room temperature and b) 14 000 pulses of 2 mW in air saturated PBS (0.2 mol.L⁻¹, pH 7) without glucose at room temperature.

Under air saturated PBS (0.2 mol.L⁻¹, pH 7) and at a concentration of glucose of 200 mmol.L⁻¹, this setup allows highly stable pulsed discharge cycles: each 3 mA-pulse delivers 2 mW for 10 ms every 10 s, at least for 5 days. This represents 40 000 charge/discharge cycles.

It is important to note that same experiments were performed after one week storage in glucose free PBS, underlining the possibility to store energy over an elevated period of time.

Conclusions

In conclusion, we showed the proof of principle of a supercapacitor/biofuel cell hybrid system that could overcome

important bottlenecks for the power supply of implantable electronic medical devices. Such a setup can clearly reduce supplemental electronics for the power management.

These CNT matrix based hybrid systems allow pulsed high power discharges that circumvent the low power output of classic glucose/O₂ biofuels.

The concept to store the generated energy within the CNT matrix also leads to a better stability of the biocatalysts which generally deteriorate under continuous discharge. Furthermore, this hybrid system overcomes the diffusion issues of glucose and oxygen to the biocatalysts and enables equilibrated charge/discharge cycles. In addition, a long term stabilization of the electron transfer rate between the enzyme and the CNT matrix was obtained. Our hybrid system is able to deliver constantly 2 mW per discharge pulse for at least 40 000 pulses during 5 days in equilibrium state. The provided performances are already sufficient to run a pacemaker and it can even be envisioned, after some optimizations, for the power supply of more energy consuming implantable devices operating with high power pulses like actuators, defibrillator, or neurostimulators. This setup represents an alternative use of enzymatic glucose biofuel cells where pulsed discharge cycles clearly improve lifetime and power output compared to continuous discharge. In contrast to classical glucose biofuel cell performance measurements applying continuous discharge that leads to local consumption of oxygen and glucose, our setup compensates this diffusion controlled energy conversion via charging the capacitance of the CNT matrix. This approach is most likely applicable for any biofuel cell devices using capacitive electrode material such as CNTs.

Acknowledgements

The authors would like to thank the Interdisciplinary Energy program of CNRS PR10-1-1 and the French National Agency for Research (ANR) Emergence-2010 EMMA-043-02 as well as the ANR program P2N-2010 Glucopac for partial financial support. The Région Rhône-Alpes is acknowledged for a PhD funding. The authors are also grateful to the scientific structure 'Nanobio' for providing facilities.

Notes and references

^a Département de Chimie Moléculaire (DCM), UMR-5250, CNRS-UJF 570 rue de la Chimie, BP 53, 38041 Grenoble, France E-mail: serge.cosnier@ujf-grenoble.fr

^b Institut Européen de Membranes (IEM) Place Eugène Bataillon, 34095 Montpellier, France.

† Footnotes should appear here. These might include comments relevant to but not central to the matter under discussion, limited experimental and spectral data, and crystallographic data.

Electronic Supplementary Information (ESI) available: [details of any supplementary information available should be included here]. See DOI: 10.1039/c000000x/

- B. E. Conway, *Electrochemical Supercapacitors*, Springer-Verlag US, 1999.
- H. D. Abruña, Y. Kiya and J. C. Henderson, *Physics Today*, 2008, **61**, 43-47.
- B. E. Conway, in *Electrochemical Supercapacitors*, Springer US, 1999, ch. 2, pp. 11-31.
- G. Wang, L. Zhang and J. Zhang, *Chem. Soc. Rev.*, 2012, **41**, 797-828.
- E. Frackowiak and F. Béguin, *Carbon*, 2001, **39**, 937-950.
- M. S. Halper and J. C. Ellenbogen, *Supercapacitors: A Brief Overview*, M. N. Group, The MITRE Corporation, McLean, Virginia, 2006.
- R. Kötz and M. Carlen, *Electrochim. Acta*, 2000, **45**, 2483-2498.
- M. F. El-Kady and R. B. Kaner, *Nat Commun*, 2013, **4**, 1475.
- M. F. El-Kady, V. Strong, S. Dubin and R. B. Kaner, *Science*, **335**, 1326-1330.
- B. E. Conway, V. Birss and J. Wojtowicz, *J. Power Sources*, 1997, **66**, 1-14.
- X. Lu, G. Wang, T. Zhai, M. Yu, J. Gan, Y. Tong and Y. Li, *Nano Lett.*, 2012, **12**, 1690-1696.
- L. P. Jarvis, T. B. Atwater and P. J. Cygan, *J. Power Sources*, 1999, **79**, 60-63.
- B. E. Conway and W. G. Pell, *J. Solid State Electrochem.*, 2003, **7**, 637-644.
- R. A. Huggins, *Solid State Ionics*, 2000, **134**, 179-195.
- U. Schröder, *Angew. Chem. Int. Ed.*, 2012, **51**, 7370-7372.
- E. Katz and K. MacVittie, *Energy & Environmental Science*, 2013, **6**, 2791-2803.
- S. Cosnier, A. Le Goff and M. Holzinger, *Electrochem. Commun.*, 2014, **38**, 19-23.
- N. Mano, F. Mao and A. Heller, *J. Am. Chem. Soc.*, 2003, **125**, 6588-6594.
- T. Miyake, K. Haneda, N. Nagai, Y. Yatagawa, H. Onami, S. Yoshino, T. Abe and M. Nishizawa, *Energy & Environmental Science*, 2011, **4**, 5008-5012.
- M. Rasmussen, R. E. Ritzmann, I. Lee, A. J. Pollack and D. Scherson, *J. Am. Chem. Soc.*, 2012, **134** 1458-1460.
- A. Szczupak, J. Halánek, L. Halámková, V. Bocharova, L. Alfonta and E. Katz, *Energy Environ. Sci.*, 2012, **5**, 8891-8895.
- L. Halámková, J. Halánek, V. Bocharova, A. Szczupak, L. Alfonta and E. Katz, *J. Am. Chem. Soc.*, 2012, **134**, 5040-5043.
- K. MacVittie, J. Halamek, L. Halamkova, M. Southcott, W. D. Jemison, R. Lobel and E. Katz, *Energy Environ. Sci.*, 2013, **6**, 81-86.
- J. A. Castorena-Gonzalez, C. Foote, K. MacVittie, J. Halánek, L. Halámková, L. A. Martinez-Lemus and E. Katz, *Electroanalysis*, 2013, **25**, 1579-1584.
- F. C. P. F. Sales, R. M. Iost, M. V. A. Martins, M. C. Almeida and F. N. Crespilho, *Lab on a Chip*, 2013, **13**, 468-474.
- A. Zebda, S. Cosnier, J.-P. Alcaraz, M. Holzinger, A. Le Goff, C. Gondran, F. Boucher, F. Giroud, K. Gorgy, H. Lamraoui and P. Cinquin, *Sci. Rep.*, 2013, **3**, 1516.
- M. Holzinger, A. Le Goff and S. Cosnier, *Electrochim. Acta*, 2012, **82**, 179-190.
- B. Reuillard, A. Le Goff, C. Agnès, A. Zebda, M. Holzinger and S. Cosnier, *Electrochem. Comm.*, 2012, **20**, 19-22.
- A. Zebda, C. Gondran, A. Le Goff, M. Holzinger, P. Cinquin and S. Cosnier, *Nature Communications*, 2011, **2**, 370.
- V. V. N. Obreja, *Physica E*, 2008, **40**, 2596-2605.
- E. P. Barrett, L. G. Joyner and P. P. Halenda, *J. Am. Chem. Soc.*, 1951, **73**, 373-380.